Restoration of a wet corrosion-resistant composite filament for material extrusion process

Restoration of a wet corrosion-resistant composite filament for material extrusion process

Alessandro Bove, Fulvio Lieske, Flaviana Calignano and Luca Iuliano
Department of Management and Production Engineering (DIGEP) – Integrated Additive Manufacturing Center (IAM), Politecnico di Torino, Turin, Italy

Abstract

Purpose – Material extrusion (MEX) is one of the most known techniques in the additive manufacturing (AM) sector to produce components with a wide range of polymeric and composite materials. Moisture causes alterations in material properties and for filaments strongly hygroscopic like nylon-based composites this means greater ease of deterioration. Drying the filament to reduce the moisture content may not be sufficient if the humidity is not controlled during printing. The purpose of this study is to achieve the recovery of a commercial nylon-based composite filament by applying process optimization using an open source MEX machine.

Design/methodology/approach – A statistical approach based on Taguchi's method allowed to achieve an ultimate tensile strength (UTS). A verification of the geometrical capabilities of the process has been performed according to the standard ISO/ASTM 52902-2019. Chemical tests were also carried out to test the resistance to corrosion in acid and basic solutions.

Findings – An UTS of 71.37 MPa was obtained, significantly higher than the value declared by the filament's manufacturer (Stratasys Inc., USA). The best configuration of process parameters leads to good geometrical deviations for flat surfaces, in a range of 0.01 and 0.38 for flatness, while cylindrical faces showed more important deviations from the nominal values. The good applicability of the material in corrosive environments has been confirmed.

Originality/value – This study examined the performance restoration potential of a nylon composite filament that was significantly affected by storage conditions. For the filament manufacturer, if the material remains in ambient air for an hour or idle in the machine for more than 24 h, the material may no longer be suitable for printing. The study highlighted that the drying of the filament must not be temporary but constant to guarantee printability, and, by acting on the process parameters, it is possible to obtain better mechanical properties than declared by the manufacturer.

Keywords Material extrusion, Composite material, Filament moisture, Corrosion resistance

Paper type Research paper

1. Introduction

In the past years, the requirements for additive manufacturing (AM) materials have become, day by day, more specific and harder to satisfy. The challenges for the realization of multi-material parts and composite materials are increasing in the research and in the industry fields, due to the recent development of the AM as a technology for the realization of functional and customized components in different panoramas. Polymeric materials were widely used in the past for the realization of prototypes, and their use was limited to few other technical applications due to the low mechanical performances, the inefficiency of the AM processes in obtaining a satisfying dimensional quality and finally the high costs of the materials and processes (Chyr and DeSimone, 2022; Jasiuk *et al.*, 2018). Nowadays, new high-performance polymers and composite materials are opening the market to new possibilities for a lot of final applications in the aerospace, energy and biomedical sectors (Calignano *et al.*, 2020; Garcia-Gonzalez *et al.*, 2015; De Leon *et al.*, 2016; El Magri *et al.*, 2021; Peluso *et al.*, 1994; Vanaei *et al.*, 2021; Wu *et al.*, 2018). Corrosion-resistant materials generate interest in multiple industrial sectors, but the design requirements for the parts are frequently highly demanding in terms of mechanical qualities and weight. In this regard, polymeric-based composite and fiber-reinforced materials present an opportunity for corrosion resistance (Prasad *et al.*, 2024; Shahid *et al.*, 2023). Among the AM processes that allow the production of parts with a large

The current issue and full text archive of this journal is available on Emerald Insight at: **https://www.emerald.com/insight/1355-2546.htm**

Rapid Prototyping Journal
Emerald Publishing Limited [ISSN 1355-2546]
[DOI 10.1108/RPJ-01-2024-0025]

Funding: Financed by the European Union – NextGenerationEU (National Sustainable Mobility Center CN00000023, Italian Ministry of University and Research Decree n. 1033 – 17/06/2022, Spoke 11 – Innovative Materials and Lightweighting). The opinions expressed are those of the authors only and should not be considered as representative of the European Union or the European Commission's official position. Neither the European Union nor the European Commission can be held responsible for them.

Received 16 January 2024
Revised 2 May 2024
10 June 2024
Accepted 21 June 2024

number of different materials containing fibers, ceramics or metal compounds (Mohd Pu'ad *et al.*, 2019), there is material extrusion (acronym MEX according to ISO/ASTM 59201). Typical polymers used for this technology are thermoplastic materials, like acrylonitrile butadiene styrene (ABS), polylactic acid (PLA) and nylon (Shanmugam *et al.*, 2021).

Thermoplastic materials are somewhat hydrophilic and absorb small amounts of moisture from the atmosphere. The strong hygroscopic behavior of the filaments used negatively affects the printability of these materials and influences the characteristics of the printed parts in terms of dimensional and geometrical properties, besides the mechanical behavior (Algarni, 2021; Aniskevich *et al.*, 2023; Quader *et al.*, 2023; Wichniarek *et al.*, 2021). In some cases, the moisture conditions of the filament may affect the intermolecular bonds, weakening the connections between the monomeric groups (Celestine *et al.*, 2020), generating internal defects and variating the glass transition temperature (Reimschuessel, 1978). The mechanical properties of a hygroscopic polymer may therefore not be adequately restored by the mere drying of the filament. Hadi *et al.* (2023) showed that reducing moisture in nylon and nylon-reinforced filaments effectively improves the mechanical properties of printed objects. However, the final outcome is also influenced by the printing temperature and process conditions.

Most MEX commercial systems do not allow to handle process parameters, and the printability of exhausted or moist filaments cannot be guaranteed after few days or weeks. Operations for the reduction of moisture in filaments are typically carried out by keeping the spool in environments with high temperatures and low relative humidities, but in some cases the chemical state of the thermoplastic material can require more specific treatments also during the printing operations (Kim *et al.*, 2016; Mohamed *et al.*, 2015; Quader *et al.*, 2023). Modifications in process parameters should be also evaluated to obtain the full recovery of a wet filament (Wichniarek *et al.*, 2021).

Especially for composite materials, modifications in the chemical state of one of the phases mixed could severely affect the reliability of the MEX process (Deb and Jafferson, 2021). Different works (Fu *et al.*, 2021; Galos *et al.*, 2021; Nagendra and Prasad, 2020; Singh and Singh, 2014) used nylon-based composite to reach enhanced characteristics with MEX process. Dispersions of metals in polymeric matrix are useful to achieve improved mechanical performances by maintaining the lightweight of parts. Ceramic materials are used to increase the corrosion resistance and the electrical insulation (Galos *et al.*, 2021).

In this study, the recovery of a wet composite filament has been carried out, by applying a Taguchi methodology for the process parameters optimization in an open-source MEX machine. Classic methods of experimental planning, e.g. factorial designs, can be used to study the influence of some process parameters on the characteristics of the parts produced. As the number of factors and the levels of each factor increase, applying a full factorial design is time-consuming, expensive and sometimes impossible. To minimize the number of tests required, it is possible to use a fractional factorial experiments (FFE). FFEs use only a portion of the total possible combinations to estimate the effects of the main factors, as well as some of the interactions. Taguchi (Gray, 1988) developed a family of FFE matrices (an orthogonal array) that has been generally adopted to optimize the design parameters and significantly reduce the overall test time and experimental costs by following a systematic approach to limit the number of experiments and tests. Various studies have utilized Taguchi's technique for MEX process (Arockiam *et al.*, 2024; Gunes *et al.*, 2024; Kam *et al.*, 2023; Li *et al.*, 2024; Uludag and Ulkir, 2024).

The modification of the global thermal conditions during the printing procedure, including the nozzle temperature and the preheating temperature of the spool, has been considered. Other MEX parameters, including deposition strategy, layer thickness and raster angle are evaluated as influencing the printability and the tensile behavior of the material. The importance of regulating thermal conditions in the MEX process is to reduce the stress conditions of the printed part, in particular for composite materials in which the different behavior of the present phases can cause the failure or damage of the final part (Amithesh *et al.*, 2023). The temperature of the building platform should be increased to reduce the warping effect, especially on high-surface layers, and the application of support material to separate the parts and the building platform provides low buckling effects. The application of preheating to the material, by keeping the filament in a temperature-controlled and humidity-controlled environment, resulted in a reduction of part defects and geometrical deviations. After the optimization of process parameters for tensile behavior of the composite material, an evaluation of the geometrical capability with the optimized parameters has been carried out and the chemical behavior of the material has been investigated by performing corrosion tests.

2. Materials and methods

2.1 Materials and moisture absorption analysis

The material used is a Diran 410MF07® (Stratasys Inc., USA), a mineral-filled material (7% by weight) made by a mixture of magnesium silicate and molybdenum disulfide in a nylon thermoplastic matrix. The diameter of the filament used is 0.75 mm. It demonstrates exceptional toughness and resistance to hydrocarbon-based chemicals. SUP4000B® filament (Stratasys Inc., USA) was used as the support material as suggested by the manufacturer. Both Diran 410MF07® and SUP4000B® are sensitive to moisture. If the material remains in ambient air for 1 h or idle in the machine for more than 24 h, the material may no longer be suitable for printing and any residue in the tubing between the bay and the head must be discarded and reloaded. Even with continuous use, the material will remain suitable for printing for a maximum of three weeks in the materials bay as indicated by the manufacturer (Stratasys, 2022). After three weeks, the material must be removed from the printer and dried before resuming printing.

To understand the state of the filament after it had been exposed in the conditions indicated as critical by the manufacturer for which it can no longer be considered suitable for printing (1 h in air and for more than 24 h in the machine), a procedure of analysis of the moisture conditions of the filament

was carried out. Thermoplastic materials are somewhat hydrophilic and, when exposed to air, absorb small amounts of moisture from the atmosphere (Choqueuse *et al.*, 1997; Weitsman and Elahi, 2000). Moisture diffusion is modeled using Fick's diffusion law with the temperature-dependent diffusion coefficient (Banjo *et al.*, 2022). Equation (1) represents the water content of the filament as a function of time according to Fick's law:

$$c(t) = c_s\left\{1 - \frac{8}{\pi^2}\sum_{k=1}^{20}\frac{1}{(2k-1)^2}\exp\left[-\frac{(2k-1)^2 D\pi^2}{d^2}t\right]\right\} \quad (1)$$

where parameters c_s, D and d represent, respectively, the water content at saturation, the diffusion coefficient and the thickness of the filament samples. The water absorption test has been performed according to Standard BS EN ISO 62:2008. Five different 25-mm-long filament samples were dried in a vacuum oven at 52C° for 48 h. The analytic balance KERN ABJ 320-4NM (Kern & Sohn GmbH, Germany), with an accuracy of ± 0.1 mg, has been used to perform the weighting procedures. The dried specimens have been weighed and then immersed in distilled water at 23 (±1)°C for 24 h, dried with a paper tissue and weighed again. The procedure was repeated for seven days, until the increase in mass of the samples was neglectable. Both c_s and D have been calculated starting from the experimental data, considering the mean values of the five different samples. The obtained model has been compared to the experimental results.

2.2 Equipment and process parameters

The aim of this study is to make the material reusable despite exposure to air and achieve the mechanical performance of the material indicated by the filament's manufacturer. To make this feasible, after an initial experimental analysis in which the filament was dried as per the manufacturer's instructions (spool into an oven at 70°C for a minimum of 4 h) without obtaining the desired results, the process conditions were varied.

The MEX machine used to produce the samples is the 3ntr A4V4 (Jdeal-Form s.r.l., Italy) equipped with three nozzles having 0.4 mm extrusion diameter. The 3ntr VENTO drying unit (Jdeal-Form s.r.l., Italy) has been used to keep the filament in low humidity conditions and to set up a pre-heating unit useful to reduce the thermal jump of the material during the process. The experimental setup used is schematized in Figure 1. The maximum nozzle temperature allowed in standard configuration is 260°C, which is high enough to extrude the support material, but insufficient to process the part material. One of the nozzle configurations has been adjusted to increase the maximum nozzle temperature up to 320°C.

The following process parameters were analyzed as it has been seen in the literature (Arockiam *et al.*, 2024; Hadi *et al.*, 2023) that they are those that most influence the mechanical characteristics: layer thickness, nozzle temperature, oven temperature, raster angle and infill style. The minimum number of experiments (MNE), according to Taguchi's method, is calculated using equation (2), where P is the number of factors and L is the number of levels considered:

$$MNE = P*(L-1)+1 = 11 \quad (2)$$

An orthogonal array L_{27} of Taguchi technique has been considered, with 27 different experimental runs and 26 degrees of freedom and 3 replications for each experiment have been performed. The factors and the levels investigated are resumed in Table 1. The optimal combination between parameters is established through a *signal-to-noise ratio* (S/N). The control factor considered in this analysis is the ultimate tensile strength (UTS), and a type of response *larger is better* is imposed. The S/N ratio is calculated using equation (3):

$$\eta_L = -10\ log_{10}\left[\frac{1}{n}\sum_{i=1}^{n}\frac{1}{y_i^2}\right] \quad (3)$$

where η_L[dB] is the S/N ratio, n is the number of repetitions of each experiment and y_i represents the observed value of the i-th experiment. The analysis of the variance (ANOVA) has been conducted using Minitab® 19 statistical software, to understand the significance of each factor in the considered analysis, with a 95% confidence interval.

KISSlicer© v1.5 was used to select parameters and perform the slicing of the samples. The samples were not produced directly on the building platform, an initial raft path was included to reduce warping and delamination effects and improve the quality of the printed material. The building orientation is parallel to the XY plane. The raft (Figure 2) was built using the respective support material. The raft part was removed manually after each sample was produced.

Each sample was produced using a double-contour strategy and variating the infill style (Figure 3). The infill density is set at 50% uniformly for all samples.

2.3 Tensile testing and geometrical characterization

The tensile test specimens have been designed according to the standard ASTM D638 – 22/Type V. The tensile tests were conducted using a tensile apparatus Aura Tensile (Easydur S.r. l., Italy) with a grips motion speed of 5 mm/min. The central section of each specimen was measured using a caliper, to calculate the stress profile and plot the results. A self-made Matlab® R2023a script was used to post-process the tensile test results and to calculate the tensile properties of the printed material.

The geometrical characterization was performed according to the standard ISO/ASTM 52902–2019, and the list of benchmarks produced is reported in Table 2. A coordinate measurement machine (CMM) DEA (Hexagon, Sweden) was used to establish the geometrical tolerances of cylindricity, concentricity, positioning for cylindrical surfaces, flatness and parallelism for horizontal and vertical flat surfaces. Linear and circular measurements were performed using a stereomicroscope Leica S9i and a caliper.

2.4 Corrosive tests

The chemical behavior of the material has been tested by evaluating the capability of a small test part of 10 × 14 × 3 cm^3 to bear the corrosive environment in 200 ml of acid solution, 0.5 M of H_2SO_4, as reported by Kumar *et al.* (Kumar *et al.*, 2017), and in 200 ml of basic solution, 0.5 M of KOH (Marzo *et al.*, 2007), for 24 h. The corrosion test in a basic solution of KOH has been

Figure 1 Schematization of the experimental setup

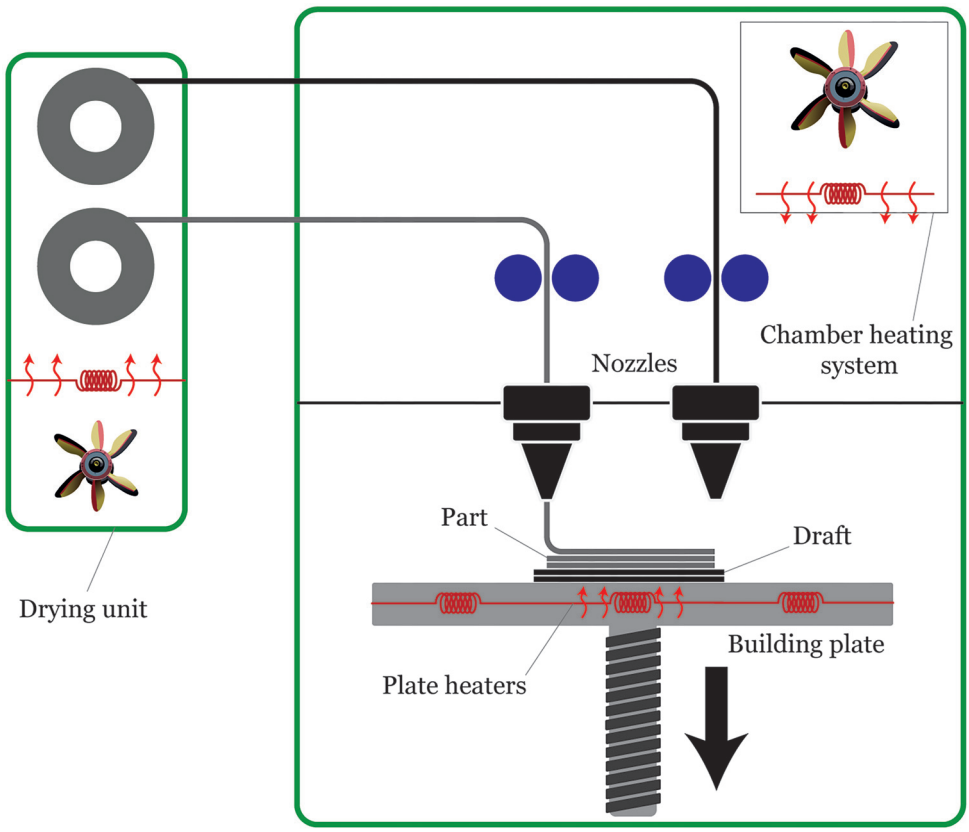

Table 1 Design of experiment: factors and their levels for the Taguchi analysis

Factors	Level −1	0	1
Layer thickness [mm]	0.1	0.2	0.3
Nozzle temperature [°C]	270	280	290
Oven temperature [°C]	55	90	115
Raster angle [deg]	0	45	90
Infill stile	Rounded	Straight	Octagonal

Figure 2 Geometries and specific dimensions of the raft part were used to support the sample during the building process

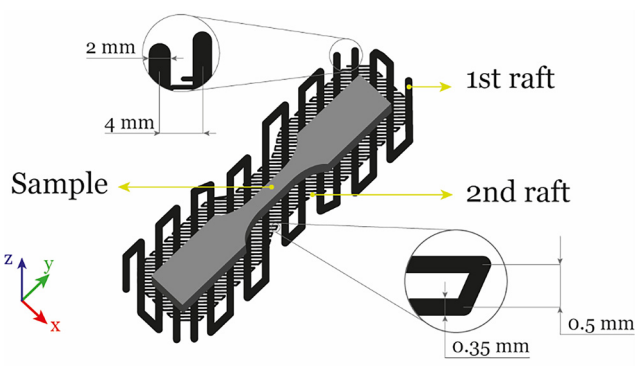

performed to verify the stability of the material as a support structure in electrochemical fuel cells. The width and the weight of the samples were measured before and after the corrosion test to establish the effectiveness of the material to keep the initial shape.

3. Results and discussions

3.1 Moisture absorption

Filament manufacturers provide a manual describing how to restore the filaments in situations where moisture levels prevent the material from being processed properly. From the manufacturer's guideline, if the material sit in ambient air for 1 h, it could cause it to become wet and unprintable. It is therefore suggested to dry the material by placing the spool in the oven at 70°C for a minimum of 4 h. The spool was left in the air for 1 h and then the printing tests were carried out. Having encountered printing difficulties, the drying procedure was carried out and a sample was subsequently printed. The test results are shown in Figure 4.

Moisture absorption analysis was then performed to get an indication of the amount of moisture absorbed by the material. The trend over time was therefore also analyzed according to Fick's law. Figure 5 shows an increase in moisture content with extended dwelling time. The c_s is measured to be around 3.39% after 170 h, while the diffusion coefficient D is 1.20 10^{-12} m^2 s^{-1}. Similar values ($D = 1.61$ 10^{-12} m^2 s^{-1}) for the diffusion coefficient are reported for a nylon composite (Markforged Onyx) by

Figure 3 The different deposition strategies analyzed on a square plate model

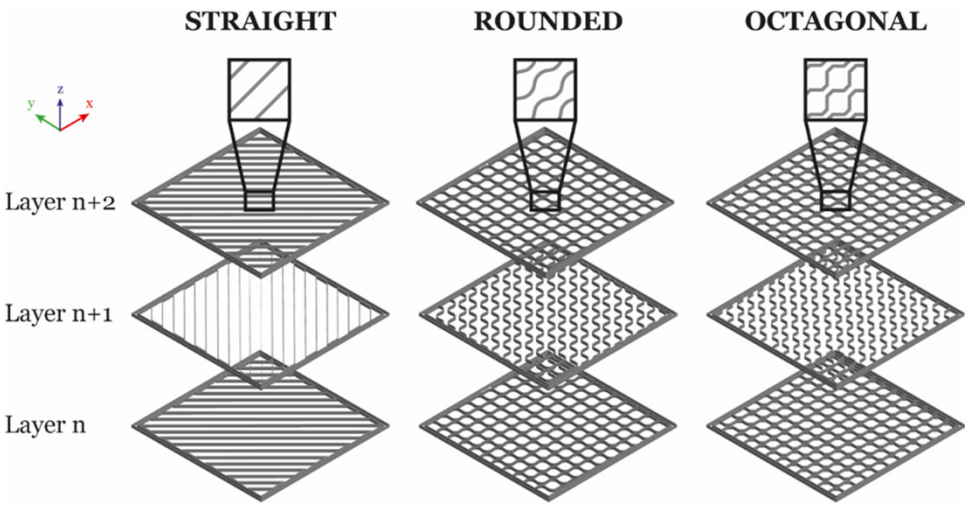

Table 2 List of the benchmarks used for the geometrical characterization

Name	Geometry measured	Measurement method	Isometric view
LA	Linear dimensions	Stereomicroscope	
RR_C	Ribs width and height, parallelism, flatness	CMM	
RR_M	Ribs width and height	Stereomicroscope	
RS_C	Slots width	Stereomicroscope	
RS_M	Slots width	Stereomicroscope	
RP_C	Pins diameters and height	Caliper	
CA_M	Cylinders diameters, center positioning, concentricity, cylindricity	CMM	

Note: Reported images of the test parts are not in scale

Banjo *et al.* (Banjo *et al.*, 2022). The hygroscopicity of the nylon matrix causes an inevitable absorption of moisture when inserting the spool into the 3D printer. This quantity, however, due to the presence of other elements in the filament is reduced compared to pure nylon (Gong *et al.*, 2022). As time increases, a certain oscillation of behavior is observed between the five samples. However, moisture absorption appears to saturate before decreasing slightly. The presence of a mixture of magnesium silicate and molybdenum disulfide in a nylon matrix appears to reduce the rate of moisture absorption, probably due to the ability of the mixture to limit the movement of water molecules.

The morphology and consistency of the extruded material are significantly influenced by the moisture content of the

Figure 4 Printing test performed after drying procedure

Figure 5 Moisture sorption measurements (marker) fitted on the predictive model of Fick's law (line)

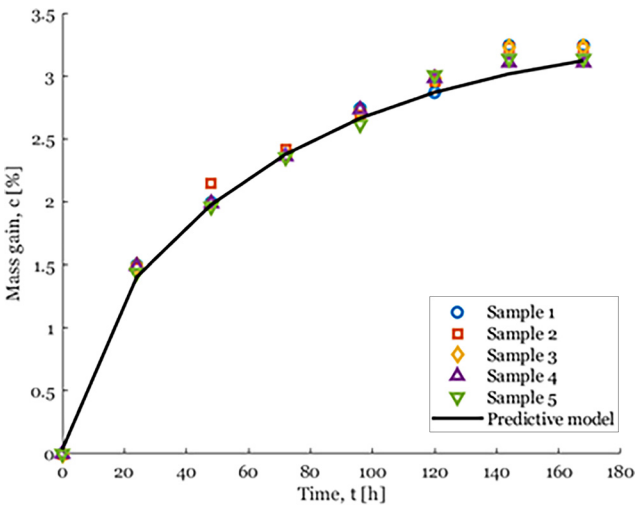

filament. The thermal behavior of the material can be significantly influenced by changes in the chemical state of the polymer, such as the glass transition temperature (Banjo *et al.*, 2022). The results highlight that if the filament is not protected from moisture, a certain variation in mass occurs in 24 h of non-use. Drying is not sufficient, since, once removed from the dryer and inserted into the 3D printer, it tends to absorb a minimal amount of humidity again ($0.5\% < c_s < 1.5\%$ within 24 h) which makes printing difficult. Therefore, it is necessary that the filament is constantly kept in the best conditions during the printing process.

3.2 Tensile properties

The results of the tensile tests are reported in Table 3 and the ANOVA performed is shown in Table 4. The response considered in the S/N ratio analysis is the average value calculated by the three different UTS values measured for each experiment replication. The infill style and layer thickness can be considered influent in affecting the tensile properties, as F-value is higher than F_{max}, evaluated for 2 degrees of freedom, and p-value is lower than 0.05 for a confidential interval of 95%. Other parameters show no significant influence in tensile behavior.

All S/N ratios are positive value (Table 5), since a *larger is better* condition has been imposed in the analysis. The delta value allows to determine the rank of significance for each factor considered: the larger the delta, the higher the significance of the factor in affecting the response.

The infill style has the biggest influence in increasing UTS, and the main effects plot (Figure 6) highlights that there is a great difference inside the categorical levels. Nagendra *et al.* (Nagendra and Prasad, 2020) found a similar behavior for the layer thickness, but no influence of the infill style was revealed, whereas the raster angle affected the tensile behavior in their model. The rounded and the octagonal are quite similar strategies, even if octagonal is preferred, while the straight strategy led to a dramatic drop in the UTS value. In contrast, the straight strategy is too many different from the others, and this behavior probably results in a strong influence in the statistical model. The layer thickness is quite influential, as the adhesion between layers depends on the height of the layers, the number of layers deposited and the thermal behavior of the fused filament. The parallelism between the drawn lines in the interaction plot reported in Figure 7 highlights the low significance of the linear interaction between the considered factors.

The most influential interaction which can be noted regards the thermal parameters, like nozzle temperature and oven temperature, and the layer thickness. A specific balance between the layer thickness and the extrusion width should be found depending on the specific process and filament. The thermal conditions which led the filament to be fused and deposited on the previous layer can affect the tangential forces which are generated during the tensile stress conditions. Globally, the UTS obtained as outcomes for all the experiments are greater in respect to the value reported in the technical datasheet of the filament manufacturer (Stratasys, 2022). The building orientation of the sample has been chosen in the XY plane, while the manufacturer's guide report results of samples XZ-oriented. This orientation choice is justified by the typical values of UTS are comparable in literature (Afrose *et al.*, 2014; Gebisa and Lemu, 2019; Lluch-Cerezo *et al.*, 2019; Patadiya *et al.*, 2020).

3.3 Geometrical characterization

The validation of the process parameters optimization conducted to improve the mechanical performances of the restored filament goes through the geometrical characterization of the printed test parts, reported in Figure 8. The optimal parameters found have been tested in terms of simple geometrical features, like flat and cylindrical surfaces.

The test outcomes highlight the minimal process resolution and dimensional capability for cylindrical and flat surfaces. Measuring the features dimensions, the linear deviation has been established, as the absolute value of the difference between the real and nominal dimension; the results of the dimensional characterization are reported in Figure 9.

Table 3 Results of the tensile tests

Experiment	Factors					UTS [MPa]
	Layer thickness	Nozzle temperature	Oven temperature	Infill style	Raster angle	
1	−1	−1	−1	−1	−1	62.50
2	−1	−1	−1	−1	0	62.16
3	−1	−1	−1	−1	1	63.67
4	−1	0	0	0	−1	62.99
5	−1	0	0	0	0	64.48
6	−1	0	0	0	1	62.09
7	−1	1	1	1	−1	68.96
8	−1	1	1	1	0	68.52
9	−1	1	1	1	1	65.04
10	0	−1	1	0	−1	63.50
11	0	−1	1	0	0	63.81
12	0	−1	1	0	1	64.44
13	0	0	−1	1	−1	69.50
14	0	0	−1	1	0	71.37
15	0	0	−1	1	1	68.95
16	0	1	0	−1	−1	67.72
17	0	1	0	−1	0	65.51
18	0	1	0	−1	1	65.79
19	1	−1	0	1	−1	67.92
20	1	−1	0	1	0	66.90
21	1	−1	0	1	1	66.11
22	1	0	1	−1	−1	62.10
23	1	0	1	−1	0	63.29
24	1	0	1	−1	1	60.88
25	1	1	−1	0	−1	52.14
26	1	1	−1	0	0	66.76
27	1	1	−1	0	1	56.13

Table 4 ANOVA Results for S/N ratios with a R^2 of 71.69%

Source	df	Seq SS	Adj MS	*F*-value	*p*-value
Layer thickness	2	1.6028	0.80141	5.37	0.016
Nozzle temperature	2	0.1142	0.05711	0.38	0.688
Oven temperature	2	0.3549	0.17744	1.19	0.330
Infill style	2	3.5111	1.75557	11.76	0.001
Raster angle	2	0.4662	0.23310	1.56	0.240
Residual error	16	2.3890			
Total	26	8.4382			

Evidence of the substantial difference between the cylindrical features and flat surfaces is shown. The RP_C artifact shows higher deviations not only in the accuracy of cylindrical pins, but also in the heights of the pins. Because of the error propagation in the layer-by-layer technique, one of the main reasons of deviations in the vertical features is losses in accuracy of the cylindrical shapes. Additionally, the CA_M artifact indicated low dimensional accuracy, suggesting that outliers may exist in the measurement data set even though the measurement's median value is significantly lower than the last quartile of the measured values. The resolution of the technique for flat vertical surfaces can be understood by comparing the RR_C and RR_M artifacts. Because of the nozzle's extrusion width, ribs in the RR_M artifact that are narrower than 0.4 mm cannot be printed, and there is a significant chance of printing error for ribs that are between 0.6 and 0.8 mm wide. Geometrical capabilities are displayed in Figure 10, and confirmations on the different behavior between flat and cylindrical shapes are evident. Vertical surfaces have more restricted deviations with respect to horizontal surfaces, this behavior is probably due to thermal deformation which occurs during and after the printing process. In general, the optimization of the thermal parameters, like the temperature of the building platform, the nozzle and chamber temperatures, allowed to keep the tolerances value for horizontal surface in a quite restricted

Table 5 S/N Ratios and delta values for factors and levels

Level	Layer thickness	Nozzle temperature	Oven temperature	Infill style	Raster angle
1	36.18	36.20	36.04	36.08	35.11
2	36.48	36.25	36.32	35.80	36.37
3	35.88	36.10	36.19	36.67	36.07
Delta	0.60	0.16	0.28	0.87	0.30
Rank	2	5	4	1	3

Figure 6 Main effects plot for S/N ratios for the evaluation of the effects of process parameters

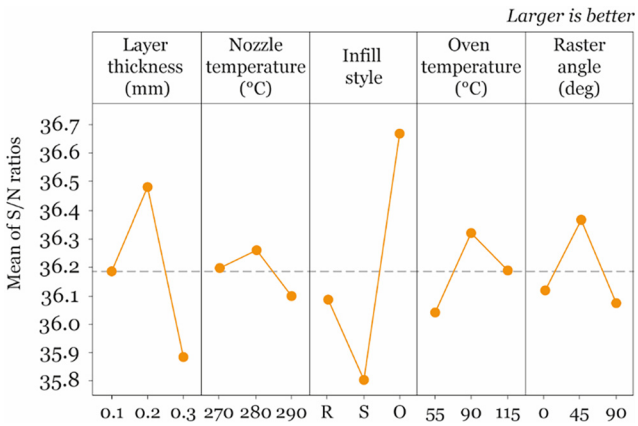

range avoiding warping effects which are typical for this kind of technology (Mazlan *et al.*, 2023).

3.4 Chemical behavior

The corrosive tests, reported in Figure 11, revealed no differences in the dimensions of the test parts before and after the 24 h immersion both in acid and basic solutions, and the width loss of both the test samples is inappreciable. Small weight gains of about 3 Wt.% were disclosed after the test in both cases, this is due to the strong hygroscopic behavior of the nylon matrix. These outcomes confirm the interest of this material for electrochemical applications, especially for the realization of customized support for conductive parts. The ability of the material to preserve the initial shape is also important in avoiding fluids leakages and pressure losses in specific environments in which the sealing should be guaranteed.

4. Conclusions

In this study the effect of drying on a nylon-based filament for the MEX process was analyzed which, if exposed to air for 1 h, could be unprintable. A nylon-based engineering thermoplastic with 7% mineral fill by weight is an interesting material in the electrochemical sector due to its chemical resistance in corrosive environments and its hygroscopic behavior in aqueous environments. The wettability of the material is an important issue for the MEX process, where a completely dry filament is required. Storing the material, once the vacuum package has been opened, in an environment that is not completely dry easily causes an increase in the moisture of the filament. Once it was highlighted that drying the filament, after being kept in the air for 1 h, an evaluation of the behavior of the material with respect to moisture absorption was carried out according to the standard BS EN ISO 62:2008. The diffusion coefficient and water content at saturation for the Diran 410MF07® filament were established. The moisture sorption behavior was compared with the Fick model. The material exhibited hygroscopic behavior and the Fick model is consistent in predicting this. The printing tests highlighted the need to keep the filament in the best conditions in terms of moisture during printing. The maximum value of UTS for a specific set of parameters reaches 71.37 MPa which is slightly higher than the value of 40 MPa reported by the manufacturer in the material data sheet. The geometrical performance of the process has been evaluated on the best configuration of process parameters resulted from the mechanical analysis, and a good

Figure 8 Printed test parts for geometrical characterization

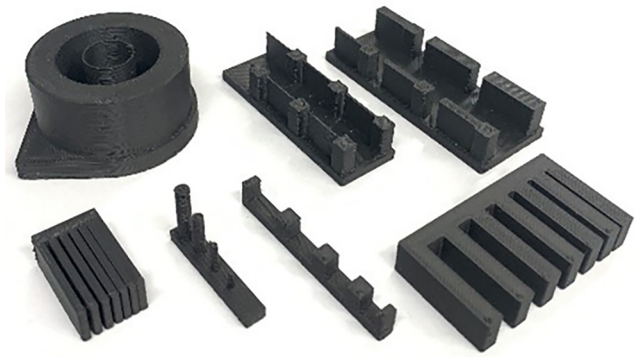

Figure 7 Interaction plot for UTS values

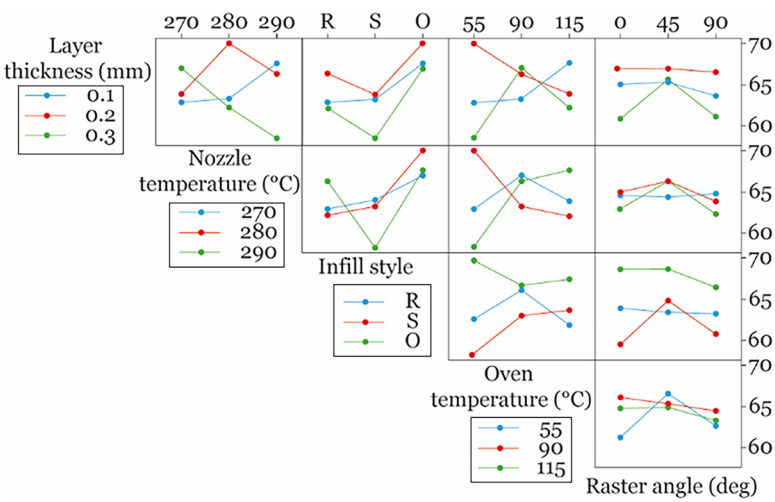

Figure 9 Dimensional deviations of the benchmark's features

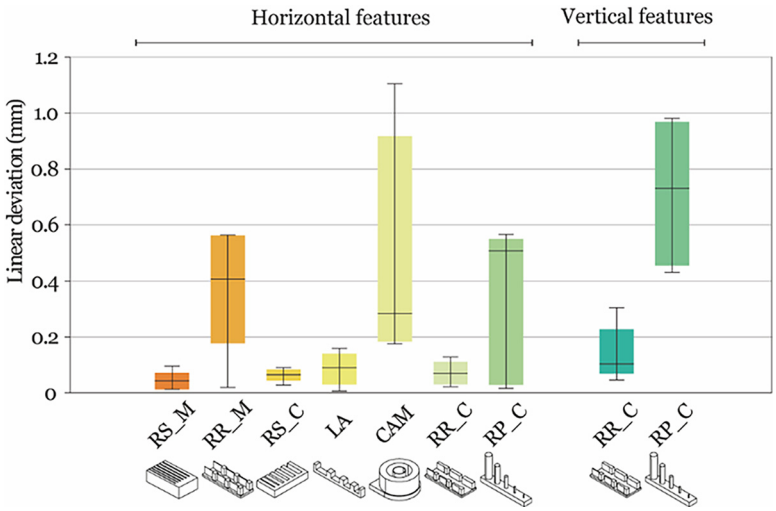

Figure 10 CMM measurements of geometrical deviations for flat and cylindrical shapes

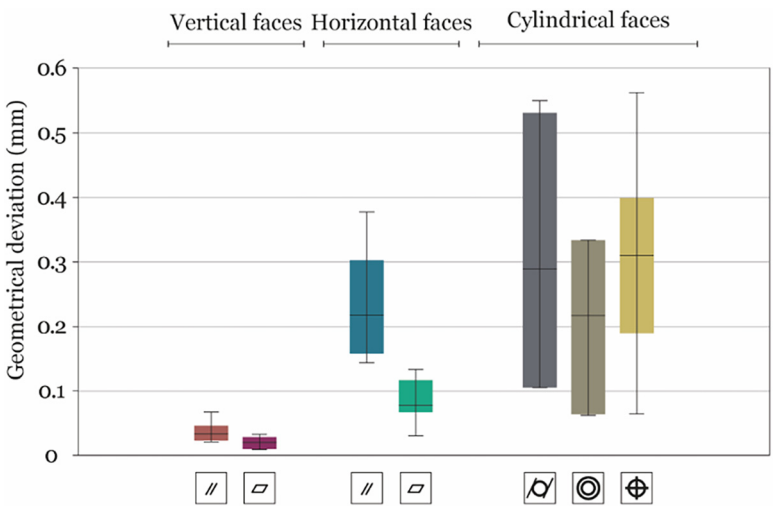

Figure 11 Experimental setup for the corrosive tests

response can be highlighted both in terms of dimensional and geometrical quality. Flatness and parallelism of vertical surfaces is contained in quite a small range, while cylindricity, positioning and concentricity are larger values, confirming the difficulty in building accurate cylindrical features. The corrosion tests gave confirmation of the good behavior of the nylon-composite material in corrosive environment both in basic and acid solutions.

References

Afrose, M.F., Masood, S.H., Nikzad, M. and Iovenitti, P. (2014), "Effects of build orientations on tensile properties of PLA material processed by FDM", *Advanced Materials Research*, Vols 1044/1045, pp. 31-34, doi: 10.4028/www.scientific.net/AMR.1044-1045.31.

Algarni, M. (2021), "The influence of raster angle and moisture content on the mechanical properties of PLA parts produced by fused deposition modeling", *Polymers*, Vol. 13 No. 2, pp. 1-12, doi: 10.3390/polym13020237.

Amithesh, S.R., Shanmugasundaram, B., Kamath, S., Adhithyan, S.S. and Murugan, R. (2023), "Analysis of dimensional quality in FDM printed nylon 6 parts", *Progress in Additive Manufacturing*, Vol. 9 No. 4, doi: 10.1007/s40964-023-00515-7.

Aniskevich, A., Bulderberga, O. and Stankevics, L. (2023), "Moisture sorption and degradation of polymer filaments used in 3D printing", *Polymers*, Vol. 15 No. 12, doi: 10.3390/polym15122600.

Arockiam, A.J., Rajesh, S., Karthikeyan, S. and Sathishkumar, G.B. (2024), "Optimization of fused deposition 3D printing parameters using Taguchi methodology to maximize the strength performance of fish scale powder reinforced PLA filaments", *International Journal on Interactive Design and Manufacturing (IJIDeM)*, doi: 10.1007/s12008-024-01853-8.

Banjo, A.D., Agrawal, V., Auad, M.L. and Celestine, A.D.N. (2022), "Moisture-induced changes in the mechanical behavior of 3D printed polymers", *Composites Part C: Open Access*, Vol. 7, p. 100243, doi: 10.1016/j.jcomc.2022.100243.

Calignano, F., Lorusso, M., Roppolo, I. and Minetola, P. (2020), "Investigation of the mechanical properties of a carbon fibre-reinforced nylon filament for 3d printing", *Machines*, Vol. 8 No. 3, doi: 10.3390/machines8030052.

Celestine, A.D.N., Agrawal, V. and Runnels, B. (2020), "Experimental and numerical investigation into mechanical degradation of polymers", *Composites Part B: Engineering*, Vol. 201, p. 108369, doi: 10.1016/j.compositesb.2020.108369.

Choqueuse, D., Davies, P., Mazéas, F. and Baizeau, R. (1997), "Aging of composites in water: comparison of five materials in terms of absorption kinetics and evolution of mechanical properties", ASTM Special Technical Publication, doi: 10.1520/stp11369s.

Chyr, G. and DeSimone, J.M. (2022), "Review of high-performance sustainable polymers in additive manufacturing", *Green Chemistry*, Vol. 25 No. 2, pp. 453-466, doi: 10.1039/d2gc03474c.

De Leon, A.C., Chen, Q., Palaganas, N.B., Palaganas, J.O., Manapat, J. and Advincula, R.C. (2016), "High performance polymer nanocomposites for additive manufacturing applications", *Reactive and Functional Polymers*, Vol. 103, pp. 141-155, doi: 10.1016/j.reactfunctpolym.2016.04.010.

Deb, D. and Jafferson, J.M. (2021), "Natural fibers reinforced FDM 3D printing filaments", *Materials Today: Proceedings*, Vol. 46, pp. 1308-1318, doi: 10.1016/j.matpr.2021.02.397.

El Magri, A., Vanaei, S. and Vaudreuil, S. (2021), "An overview on the influence of process parameters through the characteristic of 3D-printed PEEK and PEI parts", *High Performance Polymers*, Vol. 33 No. 8, pp. 862-880, doi: 10.1177/09540083211009961.

Fu, X., Zhang, X. and Huang, Z. (2021), "Axial crushing of nylon and Al/nylon hybrid tubes by FDM 3D printing", *Composite Structures*, Vol. 256, p. 113055, doi: 10.1016/j.compstruct.2020.113055.

Galos, J., Hu, Y., Ravindran, A.R., Ladani, R.B. and Mouritz, A. P. (2021), "Electrical properties of 3D printed continuous carbon fibre composites made using the FDM process", *Composites Part A: Applied Science and Manufacturing*, Vol. 151, p. 106661, doi: 10.1016/j.compositesa.2021.106661.

Garcia-Gonzalez, D., Rusinek, A., Jankowiak, T. and Arias, A. (2015), "Mechanical impact behavior of polyether-ether-ketone (PEEK)", *Composite Structures*, Vol. 124, pp. 88-99, doi: 10.1016/j.compstruct.2014.12.061.

Gebisa, A.W. and Lemu, H.G. (2019), "Influence of 3D printing FDM process parameters on tensile property of ULTEM 9085", *Procedia Manufacturing*, Vol. 30, pp. 331-338, doi: 10.1016/j.promfg.2019.02.047.

Gong, H., Runzi, M., Wang, Z. and Wu, L. (2022), "Impact of moisture absorption on 3D printing nylon filament", *Solid Freeform Fabrication 2022: Proceedings of the 33rd Annual International Solid Freeform Fabrication Symposium – An Additive Manufacturing Conference*.

Gray, C.T. (1988), "Introduction to quality engineering: designing quality into products and processes, G. Taguchi, Asian productivity organization, 1986. Number of pages: 191. Price: $29 (U.K.)", *Quality and Reliability Engineering International*, Vol. 4 No. 2, doi: 10.1002/qre.4680040216.

Gunes, S., Ulkir, O. and Kuncan, M. (2024), "Application of artificial neural network to evaluation of dimensional accuracy of 3D-printed polylactic acid parts", *Journal of Polymer Science*, Vol. 62 No. 9, pp. 1864-1889, doi: 10.1002/pol.20230876.

Hadi, A., Kadauw, A. and Zeidler, H. (2023), "The effect of printing temperature and moisture on tensile properties of 3D printed glass fiber reinforced nylon 6", *Materials Today: Proceedings*, Vol. 91, pp. 48-55, doi: 10.1016/j.matpr.2023.04.641.

Jasiuk, I., Abueidda, D.W., Kozuch, C., Pang, S., Su, F.Y. and McKittrick, J. (2018), "An overview on additive manufacturing of polymers", *JOM*, Vol. 70 No. 3, pp. 275-283, doi: 10.1007/s11837-017-2730-y.

Kam, M., İpekçi, A. and Şengül, Ö. (2023), "Investigation of the effect of FDM process parameters on mechanical properties of 3D printed PA12 samples using Taguchi method", *Journal of Thermoplastic Composite Materials*, Vol. 36 No. 1, pp. 307-325, doi: 10.1177/08927057211006459.

Kim, E., Shin, Y.J. and Ahn, S.H. (2016), "The effects of moisture and temperature on the mechanical properties of additive manufacturing components: fused deposition modeling", *Rapid Prototyping Journal*, Vol. 22 No. 6, pp. 887-894, doi: 10.1108/RPJ-08-2015-0095.

Kumar, S., Vashisht, H., Olasunkanmi, L.O., Bahadur, I., Verma, H., Goyal, M., Singh, G., *et al.* (2017), "Polyurethane based triblock copolymers as corrosion inhibitors for mild steel in 0.5 M H2SO4", *Industrial & Engineering Chemistry Research*, Vol. 56 No. 2, pp. 441-456, doi: 10.1021/acs.iecr.6b03928.

Li, Z., Liu, Y., Liang, Z. and Liu, Y. (2024), "The influence of fused deposition modeling parameters on the properties of PA6/PA66 composite specimens by the Taguchi method and analysis of variance", *3D Printing and Additive Manufacturing*, Vol. 11 No. 2, pp. e773-e786, doi: 10.1089/3dp.2022.0306.

Lluch-Cerezo, J., Benavente, R., Meseguer, M.D. and Gutiérrez, S.C. (2019), "Study of samples geometry to analyze mechanical properties in fused deposition modeling process (FDM)", *Procedia Manufacturing*, Vol. 41, pp. 890-897, doi: 10.1016/j.promfg.2019.10.012.

Marzo, F.F., Pierna, A.R., Barranco, J., Vara, G., Perez, A. and Gómez-Acebo, T. (2007), "Optimization of the microstructure and corrosion resistance of finemet type alloys in KOH solutions", *Journal of Non-Crystalline Solids*, Vol. 353 Nos 8/10, pp. 875-878, doi: 10.1016/j.jnoncrysol.2006.12.057.

Mazlan, S.N.H., Abdul Kadir, A.Z., Alkahari, M.R. and Land, T. K. (2023), "Accuracy evaluation of thin wall features fabricated by fused deposition modeling using reinforced composite materials", *Progress in Additive Manufacturing*, Vol. 8 No. 6, pp. 1357-1366, doi: 10.1007/s40964-023-00403-0.

Mohamed, O.A., Masood, S.H. and Bhowmik, J.L. (2015), "Optimization of fused deposition modeling process parameters: a review of current research and future prospects", *Advances in Manufacturing*, Vol. 3 No. 1, pp. 42-53, doi: 10.1007/s40436-014-0097-7.

Mohd Pu'ad, N.A.S., Abdul Haq, R.H., Mohd Noh, H., Abdullah, H.Z., Idris, M.I. and Lee, T.C. (2019), "Review on the fabrication of fused deposition modelling (FDM) composite filament for biomedical applications", *Materials Today: Proceedings*, Vol. 29, pp. 228-232, doi: 10.1016/j.matpr.2020.05.535.

Nagendra, J. and Prasad, M.S.G. (2020), "FDM process parameter optimization by Taguchi technique for augmenting the mechanical properties of nylon–aramid composite used as filament material", *Journal of The Institution of Engineers (India): Series C*, Vol. 101 No. 2, pp. 313-322, doi: 10.1007/s40032-019-00538-6.

Patadiya, N.H., Dave, H.K. and Rajpurohit, S.R. (2020), "Effect of build orientation on mechanical strength of FDM printed PLA BT", in Shunmugam, M.S. and Kanthababu, M. (Eds), *Advances in Additive Manufacturing and Joining*, Springer Singapore, Singapore, pp. 301-307.

Peluso, G., Petillo, O., Ambrosio, L. and Nicolais, L. (1994), "Polyetherimide as biomaterial: preliminary in vitro and in vivo biocompatibility testing", *Journal of Materials Science: Materials in Medicine*, Vol. 5 Nos 9/10, pp. 738-742, doi: 10.1007/BF00120367.

Prasad, P.S., Guerrero, J.D.M. and Kumar, P. (2024), "Natural and synthetic Fiber-Filled polymer composites used as anticorrosive materials", in Sethi, S.K., Gupta, H.S. and Verma, A. (Eds.), *Polymer Composites: From Computational to Experimental Aspects*, Springer Nature, Singapore, Singapore, pp. 181-202, doi: 10.1007/978-981-97-0888-8_9.

Quader, R., Dramko, E., Grewell, D., Randall, J. and Narayanan, L.K. (2023), "Characterizing the effect of filament moisture on tensile properties and morphology of fused deposition modeled polylactic acid/polybutylene succinate parts", *3D Printing and Additive Manufacturing*, Vol. 11 No. 3, doi: 10.1089/3dp.2022.0222.

Reimschuessel, H.K. (1978), "Relationships on the effect of water on glass transition temperature and Young's modulus of nylon 6", *Journal of Polymer Science: Polymer Chemistry Edition*, Vol. 16 No. 6, pp. 1229-1236, doi: 10.1002/pol.1978.170160606.

Shahid, M.D., Hashim, M.H.M., Mustafa, W.A.W., Fadzil, N.M. and Muda, M.F. (2023), "Finite element analysis (FEA) of Fiber-Reinforced polymer (FRP) repair performance for subsea oil and gas pipelines: the recent brief review (2018-2022)", *Journal of Advanced Research in Applied Sciences and Engineering Technology*, Vol. 32 No. 3, pp. 366-379, doi: 10.37934/araset.32.3.366379.

Shanmugam, V., Pavan, M.V., Babu, K. and Karnan, B. (2021), "Fused deposition modeling based polymeric materials and their performance: a review", *Polymer Composites*, Vol. 42 No. 11, pp. 5656-5677, doi: 10.1002/pc.26275.

Singh, R. and Singh, S. (2014), "Development of nylon based FDM filament for rapid tooling application", *Journal of The Institution of Engineers (India): Series C*, Vol. 95 No. 2, pp. 103-108, doi: 10.1007/s40032-014-0108-2.

Stratasys (2022), "Diran 410MF07 material guide", available at: www.stratasys.com/siteassets/mg_fdm_diran-material-user-guide_0622a.pdf?v=49c594

Uludag, M. and Ulkir, O. (2024), "Optimizing surface roughness in soft pneumatic gripper fabricated via FDM: experimental investigation using Taguchi method", *Multidiscipline Modeling in Materials and Structures*, Vol. 20 No. 1, pp. 211-225, doi: 10.1108/MMMS-09-2023-0313.

Vanaei, S., Parizi, M.S., Vanaei, S., Salemizadehparizi, F. and Vanaei, H.R. (2021), "An overview on materials and techniques in 3D bioprinting toward biomedical application", *Engineered Regeneration*, Vol. 2, pp. 1-18, doi: 10.1016/j.engreg.2020.12.001.

Weitsman, Y.J. and Elahi, M. (2000), "Effects of fluids on the deformation, strength and durability of polymeric composites – an overview", *Mechanics Time-Dependent Materials*, Vol. 4, pp. 107-126, doi: 10.1023/A:1009838128526.

Wichniarek, R., Hamrol, A., Kuczko, W., Górski, F. and Rogalewicz, M. (2021), "ABS filament moisture compensation possibilities in the FDM process", *CIRP Journal of Manufacturing Science and Technology*, Vol. 35, pp. 550-559, doi: 10.1016/j.cirpj.2021.08.011.

Wu, H., Krifa, M. and Koo, J.H. (2018), "Rubber (SEBS-g-MA) toughened Flame-Retardant polyamide 6: microstructure, combustion, extension, and izod impact behavior", *Polymer-Plastics Technology and Engineering*, Vol. 57 No. 8, pp. 727-739, doi: 10.1080/03602559.2017.1344856.

Corresponding author

Flaviana Calignano can be contacted at: flaviana.calignano@polito.it